Lawrence Berkeley National Laboratory
Lawrence Berkeley National Laboratory

Title
Creep properties of Pb-free solder joints

Permalink
https://escholarship.org/uc/item/2dn704z0

Authors
Song, H.G.
Morris Jr., J.W.
Hua, F.

Publication Date
2002-04-01

eScholarship.org Powered by the California Digital Library
University of California

Creep Properties of Pb-Free Solder Joints

H.G Song[1], J.W. Morris, Jr.[1] and F. Hua[2]

[1]Department of Materials Science and Engineering, University of California, Berkeley, CA 94720

and Center for Advanced Materials, Lawrence Berkeley National Laboratory

[2]Materials Technology Operation, Intel Corporation

Santa Clara, CA 95054

Abstract

This paper describes the creep behavior of three Sn-rich solders that have become candidates for use in Pb-free solder joints: Sn-3.5Ag, Sn-3Ag-0.5Cu and Sn-0.7Cu. The three solders show the same general behavior when tested in thin joints between Cu and Ni/Au metallized pads at temperatures between 60 and 130°C. Their steady-state creep rates are separated into two regimes with different stress exponents (n). The low-stress exponents range from ~3-6, while the high-stress exponents are anomalously high (7-12). Strikingly, the high-stress exponent has a strong temperature dependence near room temperature, increasing significantly as the temperature drops from 95 to 60ºC. The anomalous creep behavior of the solders appears to be due to the dominant Sn constituent. Joints of pure Sn have stress exponents, n, that change with stress and temperature almost exactly like those of the Sn-rich solder joints. Research on creep in bulk samples of pure Sn suggests that the anomalous temperature dependence of the stress exponent may show a change in the dominant mechanism of creep. Whatever its

source, it has the consequence that conventional constitutive relations for steady-state creep must be used with caution in treating Sn-rich solder joints, and qualification tests that are intended to verify performance should be carefully designed.

Introduction

Legislative and marketing pressures from many sources are forcing the gradual adoption of Pb-free solders in microelectronics. The design of reliable joints with these solder compositions is made difficult by the lack of prior service experience and by the shortage of probative mechanical property data.

Thermal fatigue is a primary threat to the reliability of solder joints. Soldered joints are thermally cycled in service, and are stressed in each thermal cycle due to inhomogeneities in the pattern of heating and the coefficient of thermal expansion. The dominant stresses tend to be in shear. Since the operating temperatures of microelectronic devices are a significant fraction of the melting temperatures of the solders used, the solders deform in high-temperature creep, and joints eventually fail by creep fatigue [1,2]. The understanding of creep behavior and creep mechanisms is fundamental to the design of reliable joints.

Many of the solder compositions that are attracting the greatest current interest are Sn-rich compositions from the Sn-Ag and Sn-Cu systems [3]. There is limited creep data for

these alloys, and a good part of that which is available was measured with bulk samples whose relevance to the behavior of solder joints is not at all clear. Our own recent work, including that reported here, was intended to address this problem by conducting high-temperature creep tests on well-characterized solder joints. In this paper we shall discuss recent results with Sn-3.5Ag, Sn-3Ag-0.5Cu and Sn-0.7Cu (wt. %), made as thin joints connecting Cu and Ni/Au metallized substrates. As we shall see, the behavior of these systems is strongly influenced by the dominant Sn phase.

Experimental Procedure

The solder compositions discussed here were made by melting 20g ingots from pure (99.999% in metallic base) elemental starting materials. After melting, the alloys were homogenized for 55hrs at 180°C, then cold rolled into foils of about 155 μm thickness.

Creep tests were done on nine-pad single shear creep specimens with the geometry shown in Fig. 1. The substrate pad size is about 1.22mm x 2.24mm. The joints were made between dissimilar substrates (as is common in industrial practice); the pad metallization on one side was Cu while that on the other side was about 4 μm electroless Ni coated with about 0.13 μm immersion Au. The solder joint thickness was fixed at 160 μm. The shear specimens were reflowed in nitrogen with a peak temperature of 235°C for Sn-3.5Ag and Sn-3Ag-0.5Cu and 245°C for Sn-0.7Cu. Samples were cooled at the rate of 2.7°C/sec, followed by aging at 160°C for 4 hours.

Creep tests were done in a dead-load creep machine. The sample is loaded with a fixed weight while its temperature is controlled by an oil bath. The creep specimen is held by frictional grips. The displacement of the grips was monitored with a Linear Voltage Displacement Transmitter (LVDT) that has a detection limit below 1 μm displacement. The shear stress is measured as load divided by the solder-substrate contact area (total area of the wetted pads). The shear strain (simple shear) is the relative displacement of the sample plates divided by solder joint thickness. Creep tests were conducted until steady state was reached and passed, and the reported creep rates were the steady-state creep rates. Samples were tested at 3 different temperatures: 60°C, 95°C and 130°C, and at 5 different load levels at each temperature.

Creep behavior

Figure 2(a-c) shows creep curves of the Sn-3Ag-0.5Cu solder joints. These are typical for the materials tested in this work. There is a fairly rapid evolution into a well-defined steady state creep, and followed by evolution into tertiary creep.

Steady state strain rates were measured as functions of stress and temperature from the linear portions of the creep curves for the three solder compositions and for identical joints of pure Sn. Log-log plots of the steady-state strain rates as functions of stress for the solder joints are given in Fig. 3(a-c). The data are ordinarily fit to constitutive equations of the Dorn form [4]:

$$\dot{\gamma} = \frac{AGb}{kT}\left[\frac{\tau}{G}\right]^{n} \exp\left[\frac{-Q}{kT}\right] \tag{1}$$

where $\dot{\gamma}$ is the shear strain rate, τ the shear stress, G the shear modulus, b the Burgers vector, Q the activation energy and kT the Boltzmann temperature. If this is done, the data divide naturally into high- and low-stress regions with different stress exponents (n) (Fig. 4), as often found for solder joints [1].

The major anomaly in the data is in the temperature dependence of the stress exponent in the high-stress regime. The stress exponent in the high-stress regime is greater than about 7 in all cases, but increases dramatically as the temperature is decreased from 95ºC to 60ºC, a range of significant technological interest. The fact that this behavior is common to all of the Sn-rich solders suggests that it is due to the Sn-rich constituent itself. This behavior is documented in Fig. 5, which compares the steady state creep rates of the solder joints to that of pure Sn joints at 95ºC. The steady-state creep behavior of Sn-0.7Cu is almost identical to that of pure Sn over this stress range. The more highly alloyed SnAg and SnAgCu solders are more creep-resistant than Sn, but have almost identical stress exponents at this temperature. Clearly, the anomalous temperature dependence of the Sn-rich solders is primarily due to the behavior of Sn itself.

Given the anomalous temperature dependence of the stress exponent it is deceptive to use the conventional Dorn equation to represent the creep data. There is no well-defined activation energy at lower temperature. Nonetheless a fit to the Dorn equation may be

useful as a first-order fit to the creep behavior over this temperature regime. For this reason the best-fit stress-exponents and activation energies are tabulated in Table 1, and compared with those for pure Sn. The best-fit activation energies cluster about 85 kJ/mole, the measured value for pure Sn. The best-fit stress exponents in the low-stress regime vary from near 3.5 (SnCu) to 6.6 (SnAgCu). In the high-stress regime they are much higher, ranging from 7.7 (Sn) to 10.7 (SnAgCu).

Discussion

The data presented here suggest that the creep behavior of Sn-rich solders is dominated by the behavior of Sn, and has an anomalous temperature dependence at temperatures slightly above room temperature. While the literature on the creep of pure Sn is not entirely consistent, there are indications of thermal anomalies in several published reports. In particular, Breen and Weertman [6], Suh, et al. [7], and Poirier [8] all noted significant changes in the creep behavior of bulk Sn at about 100ºC, evidenced by a change in the activation energy for steady-state creep from above 100 to below 50 kJ/mole. Frenkel, et al. [9] and Mohamed, et al. [10] confirm the high-temperature value of the activation energy, while Adeva, et al. [11], Mathew, et al. [12] and others [13,14] have measured much lower activation energies at lower temperature. The measured activation energies are close to those for lattice diffusion (~100 kJ/mole [15,16]) and dislocation pipe diffusion (40-60 kJ/mole [11,17,18]) suggesting that the dominant activation step changes from lattice to pipe diffusion as the temperature drops.

While the change in creep behavior with temperature complicates the understanding and prediction of creep in Sn-rich solders, the relative insensitivity of the creep behavior to composition simplifies it. Eutectic Sn-0.7Cu is very close to Sn in its creep behavior, while the addition of Ag hardens the solder without dramatically changing the stress exponents or activation energies, that is, the predominant effect is on the pre-exponential factor, A, in eq. (1).

The stress exponents reported in the literature for Sn and Sn-rich solders scatter widely, from near 5 (Breen and Weertman [6], Darveaux and Banerji [19]) to 10-11 (Yang, et al. [20], Mavoori, et al. [21]). In the present work, this whole range of stress exponents appears in the same data set, depending on the stress range and the temperature. In particular, the data reported here show a systematic change in stress exponent with stress and temperature for all of the solders studied. It is not yet clear to what extent this systematic variation explains the wide variations in reported results.

Finally, we should note the tetragonal crystal structure of Sn, which causes anisotropy in its mechanical properties. The creep behavior of Sn and Sn-rich joints may, therefore, be affected by crystallographic texture, particularly in as-solidified solder joints. The crystallographic texture of the joints studied here is not yet known.

Conclusion

The creep behavior of Sn and Sn-rich solder joints in shear is a complex function of stress and temperature. In particular, the stress exponent that governs steady-state creep has different values in the low- and high-stress regimes. The stress exponent at high stress changes significantly with temperature as temperature drops below about 100ºC, and reaches anomalously high values (n = 10-11) at lower temperatures. These anomalous features suggest that qualification and design verification tests for Sn-rich solder joints should use geometries and conditions as near as possible to those anticipated in service, until further research clarifies how this complex creep behavior can be understood metallurgically and treated analytically.

Acknowledgments

This research was supported by Intel Corporation and by the Director, Office of Science, Office of Basic Energy Sciences, Division of Materials Sciences and Engineering, of the U.S. Department of Energy under Contract No. DE-AC03-76SF00098.

References

1. J.W. Morris, Jr. and H.L. Reynolds, *Design and Reliability of Solders and Solder Interconnections*, ed. R.K. Mahidhara, D.R. Frear, S.M.L. Sastry, K.L. Murty, P.K. Liaw, and W. Winterbottom (Warrendale, PA: TMS Soc., 1997), p. 49.

2. M.C. Shine and L.R. Fox, *Low Cycle Fatigue, ASTM STP 942*, ed. H.D. Solomon, G.R. Halford, L.R. Kaisand, and B.N. Leis (Philadelphia, PA: 1988), p. 588.

3. K. Suganuma, *MRS Bulletin*, 26 (2001), p. 880.

4. J.E.Bird, A.K. Mukherjee, and J.E. Dorn, *Quantitative Relation Between Properties and Microstructure*, ed. D.G. Brandon and A. Rosen (Jerusalem, Israel: Israel Univeristy Press, 1969), p. 255.

5. Z. Guo, Y-H Pao, and H. Conrad, *J. Electron. Packag.*,117 (1995), p. 101.

6. J.E. Breen and J. Weertman, *Trans. AIME*, 203 (1955), p. 1230.

7. S.H. Suh, J.B. Cohen, and J. Weertman, *Metall. Trans. A*, 14A (1983), p. 117.

8. J.P. Poirier, *Acta Metall.,* 26 (1978), p. 629.

9. R.E. Frenkel, O.D. Sherby, and J.E. Dorn, *Acta Metall.,* 3 (1955), p. 470.

10. F.A. Mohamed, K.L. Murty, and J.W.Morris, Jr., *Metall. Trans.,* 4 (1973), p. 935.

11. P. Adeva, G. Caruana, O.A. Ruano, and M. Torralba, *Mater. Sci. Eng. A*, A194 (1995), p. 17.

12. M.D. Mathew, S. Movva, H. Yang, and K.L. Murty, *Creep Behaviors of Advanced Materials for the 21st Century*, ed. R.S. Mishra, A.K. Mukherjee, and K.L. Murty (Warrendale, PA: TMS Soc., 1999), p. 51.

13. L. Rotherham, A.D.N. Smith, and G.B. Greenough, *J. Inst. Met.,* 79 (1951), p. 439.

14. R. J. McCabe and M.Fine, *JOM*, 52 (2000), p. 33.

15. J.D. Meakin and E. Klokholm, *Trans. Met. Soc. AIME*, 218 (1960), p. 463.

16. C. Coston and N.H. Nachtrieb, *J. Phys. Chem.*, 68 (1964), p. 2219.

17. V.I. Igoshev and J.I. Kleiman, *J. Electron. Mater.,* 29 (2000), p. 244.

18. T. Reinikainen and J. Kivilahti, *Metall. Mater. Trans. A,* 30A (1999), p. 123.

19. R. Darveaux and K. Banerji, *IEEE Trans. Comp. Hybrids, Manuf. Technol.,* 15 (1993), p. 1013.

20. H. Yang, P. Deane, P. Magill, and K.L. Murty, *Proc. 46th Electr. Comp. Technol. Conf.* (New York, NY: IEEE, 1996), p. 1136.

21. H. Mavoori, J. Chin, S. Vaynman, B. Moran, L. Keer, and M. Fine, *J. Electron. Mater.,* 26 (1997), p. 783.

Figure and Table Captions

Figure 1. Schematic diagram of the specimen geometry.

Figure 2. Creep Curves of Sn-3Ag-0.5Cu at (a) 60°C, (b) 95°C, and (c) 130°C.

Figure 3. Log-log plots of the steady-state strain rate as a function of stress for the solder joints with composition (a) Sn-3.5Ag, (b) Sn-3Ag-0.5Cu, and (c) Sn-0.7Cu.

Figure 4. Typical log-log plot of $(d\gamma/dt)(T/G)\exp(Q/kT)$ versus τ/G

Figure 5. The steady-state strain rates of all alloy solder joints and pure Sn joints at 95°C.

Table 1. The best-fit stress exponents (n) and activation energies (Q) for creep of solder joints. The temperature dependence of the shear modulus of pure Sn in ref. 5 was used for the data analysis of all solder joints.

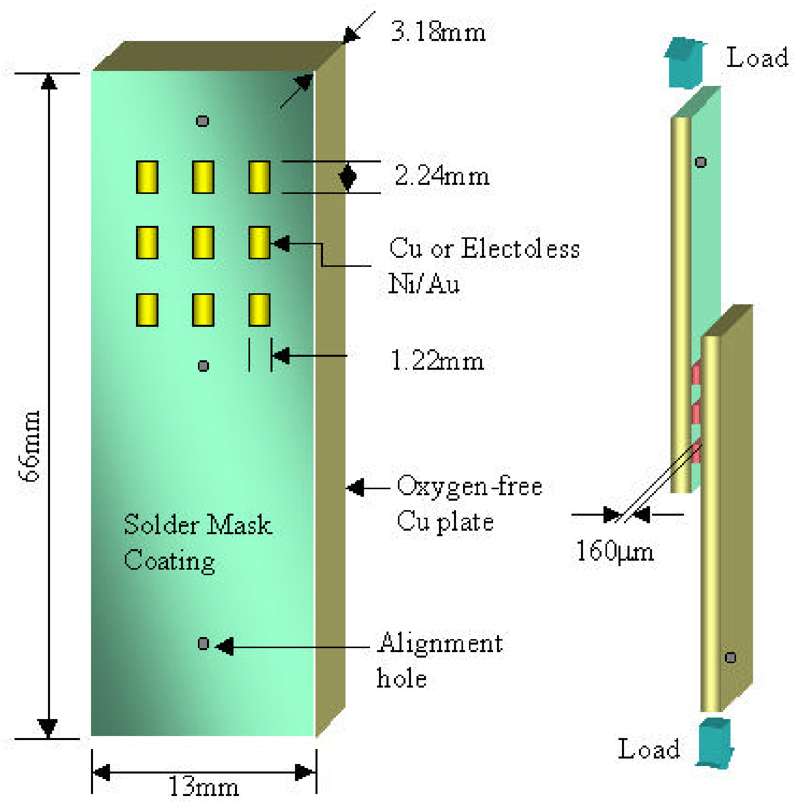

Figure 1. Schematic diagram of the specimen geometry.

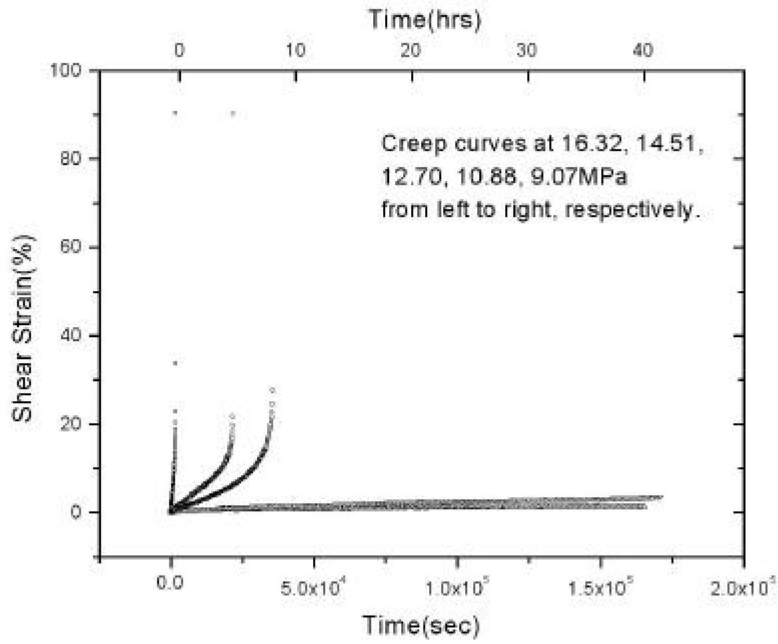

(a) 60°C

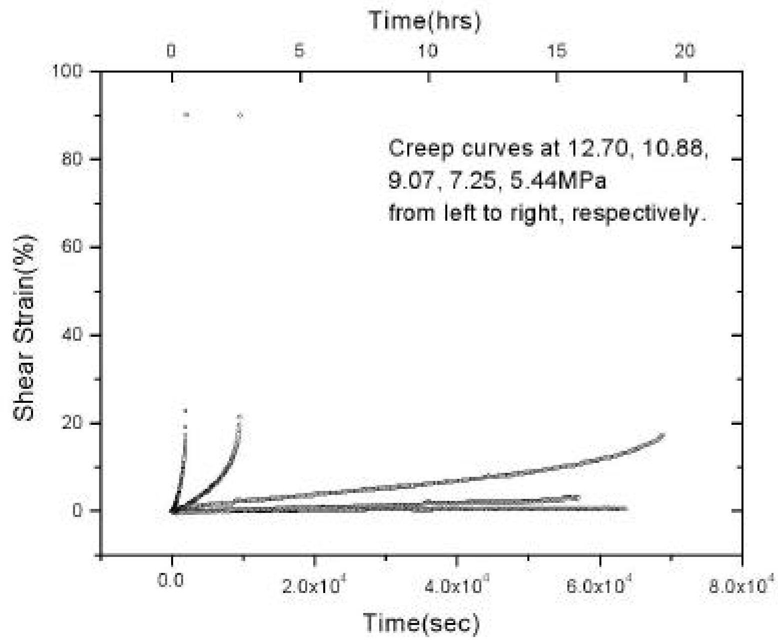

(b) 95°C

Figure 2. Creep Curves of Sn-3Ag-0.5Cu at (a) 60°C, (b) 95°C, and (c) 130°C.

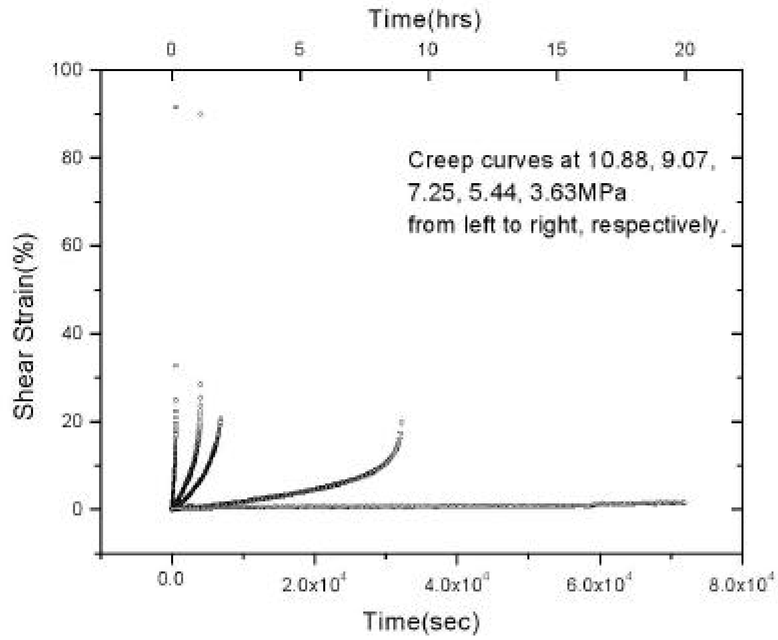

(c) 130°C

Figure 2. Continued.

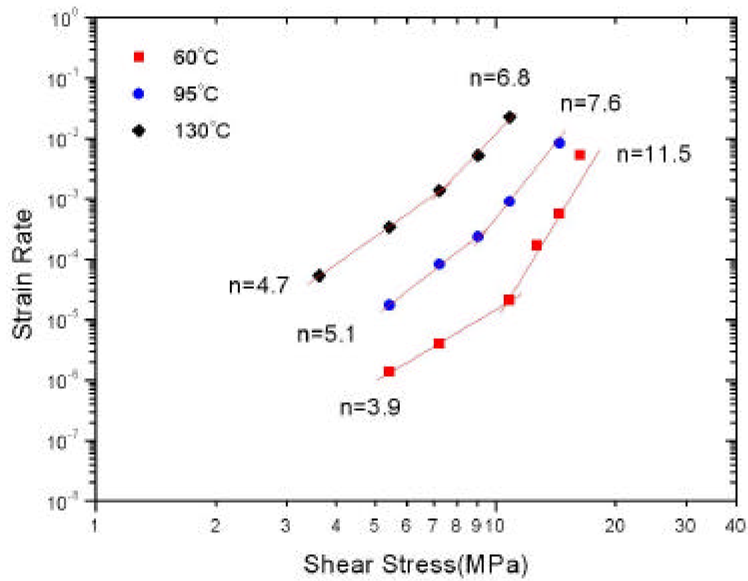

(a) Sn-3.5Ag

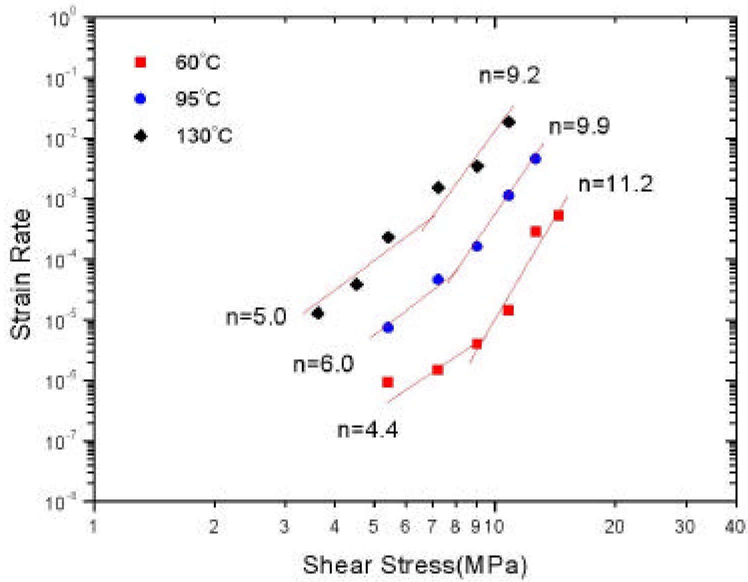

(b) Sn-3Ag-0.5Cu

Figure 3. Log-log plots of the steady-state strain rate as a function of stress for the solder joints with composition (a) Sn-3.5Ag, (b) Sn-3Ag-0.5Cu, and (c) Sn-0.7Cu.

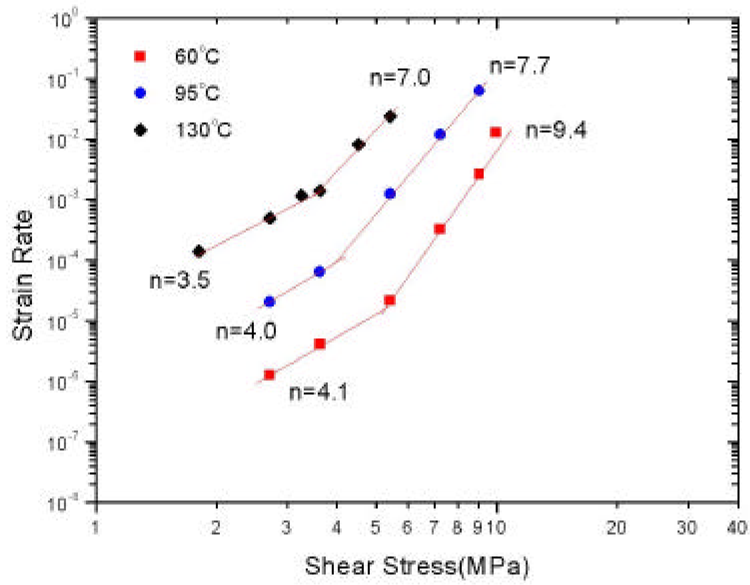

(c) Sn-0.7Cu

Figure 3. Continued.

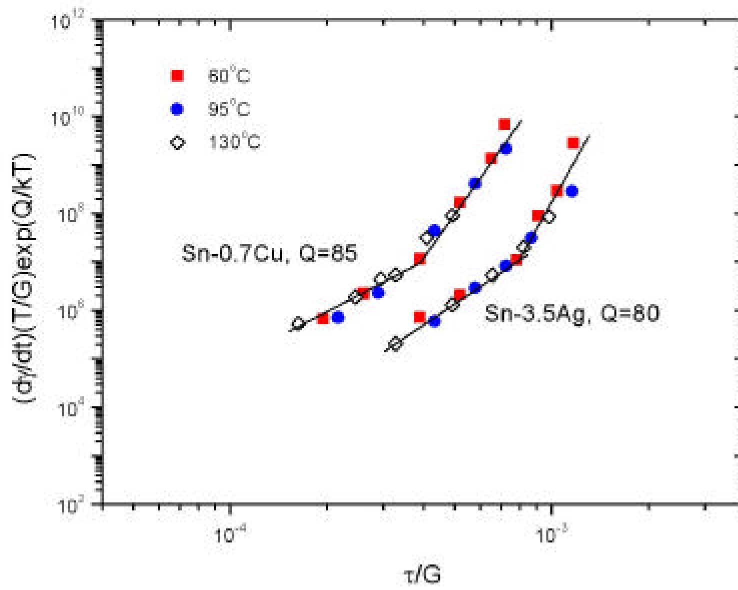

Figure 4. Typical log-log plot of (dγ/dt)(T/G)exp(Q/kT) versus τ/G

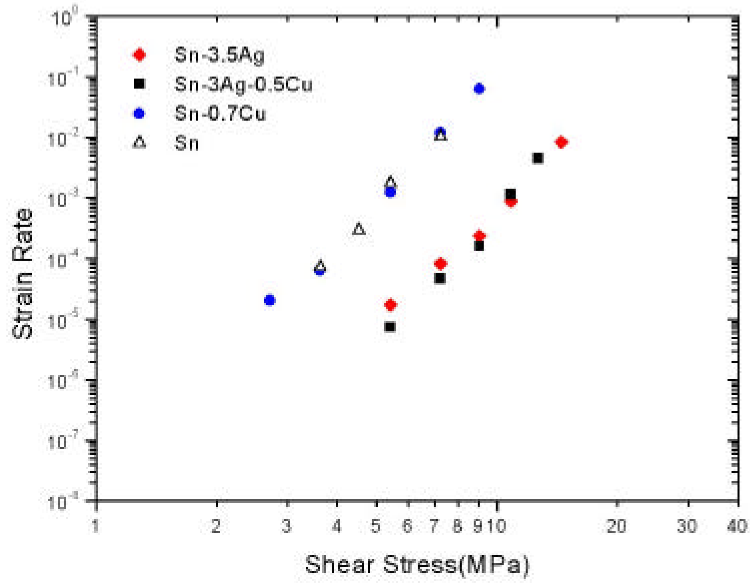

Figure 5. The steady-state strain rates of all alloy solder joints and pure Sn joints at 95°C.

Table 1. The best-fit stress exponents (n) and activation energies (Q) for creep of solder joints. The temperature dependence of the shear modulus of pure Sn in ref. 5 was used for the data analysis of all solder joints

	n		Q(KJ/mole)	
	Low τ/G	High τ/G	Low τ/G	High τ/G
Sn-Ag	4.5	10.6	80	75
Sn-Ag-Cu	6.6	10.7	95	75
Sn-Cu	3.5	8.9	90	85
Sn	5.8	7.7	85	65